Journal of Research in Science and Engineering (JRSE)
ISSN: 1656-1996 Volume-8, Issue-1, January 2026
DOI: 10.53469/jrse.2026.08(01).03

Dynamic Response Analysis of Debris Flow Impacting Bridge Piers Based on the SPH-FEM Coupling Method

Nian Li[1], Chen Cao[1], Fei Wang[2], Tie Jin[1]

[1]College of Construction Engineering, Jilin University, Changchun 130012, Jilin, China
[2]China Railway Design Corporation, Tianjin 300251, Tianjin, China

Abstract: ***Debris flows pose a serious threat to railway bridge piers in mountainous areas due to their high density, strong impact force, and long-duration dynamic loading. To investigate the dynamic response of bridge piers under debris flow impacts, this study adopts a coupled Smoothed Particle Hydrodynamics–Finite Element Method (SPH–FEM). The SPH method models the large deformation and solid–liquid two-phase behavior of debris flow, while FEM simulates the structural response of bridge piers. Refined mesh modeling and elastoplastic constitutive models are applied to capture fluid–structure interaction. Simulations are conducted for 20-year and 50-year return period scenarios, focusing on impact force evolution and energy transfer. Results show that the impact process consists of three stages: initial contact, peak impact, and decay–accumulation. Bridge piers experience both instantaneous peak loads and sustained residual loads, with energy dissipation closely related to structural plastic deformation.***

Keywords: Mining Areas, Debris-Flow, SPH-FEM Coupling Method, Bridge Pier, Dynamic Response**.**

1. Introduction

Railway bridge piers, as an important component of transportation infrastructure, often face the threat of debris flow impact in mountainous areas or regions prone to geological disasters. Debris flow, as a typical multiphase mixture geological disaster, has a significantly complex destructive mechanism [1]. In terms of material composition, debris flow usually contains a large amount of solid-liquid mixed high-density fluid, and this special material composition endows it with both fluid movement characteristics and solid impact characteristics [2]. Moreover, the debris flow impact process often lasts for tens of seconds to several minutes, and this long-term dynamic load effect can cause cumulative damage to the structure [3].

In current engineering practice, there are still many key issues to be solved regarding the dynamic response of bridge piers under debris flow impact loads. Traditional hydraulics calculation methods are difficult to accurately describe the complex process of interaction between debris flow, a high-density fluid, and structures [4]; while conventional finite element methods encounter difficulties such as mesh distortion when dealing with large deformation problems [5]. Additionally, existing research mostly focuses on the structural response under static loads or regular wave loads, and there is still insufficient understanding of the failure mechanism of bridge piers under the special impact load of debris flow. Particularly in aspects such as energy conversion mechanisms, damage accumulation processes, and structural failure modes, there is a lack of systematic research results.

Based on the above background, this paper adopts the SPH-FEM coupled numerical simulation method, combined with refined mesh modeling technology and elastoplastic analysis theory, to deeply explore the dynamic response laws of railway bridge piers under debris flow impact. The research results will provide theoretical support for the anti-impact design of railway bridge piers in mountainous areas and have important practical value for enhancing the disaster prevention and mitigation capabilities of major transportation infrastructure. At the same time, the analysis framework and method system established in this paper can also provide useful references for the research on the resistance of other types of structures to geological disaster impacts.

This paper systematically conducts the following three aspects of research work around the dynamic response analysis of railway bridge pier infrastructure:

1) Refined mesh modeling of debris flow gully terrain and coupling analysis of high-density fluid motion.

2) Rigid collision simulation of 1:1 original models of bridge piers and their ancillary structures.

3) Elastoplastic body collision analysis technology.

The research results show that the debris flow impact process can be divided into three stages: initial contact, peak impact, and attenuation accumulation. The dynamic response of the bridge pier presents the coexistence of instantaneous peak loads and long-term residual loads, and its energy dissipation mechanism is closely related to the plastic deformation of the structure.

2. Overview of the Study Area

The study area is located in Yongding District, Zhangjiajie City. It is situated in the central part of Zhangjiajie, with the valley entrance located at E: 110°25′11.69″, N: 29°12′57.62″. The average annual temperature over the years is 16.8℃, the average annual sunshine duration is 1450 hours, and the average annual precipitation is 1497 millimeters.

The overall shape of the study area is irregular and leaf-like, trending southwest to east. The height difference from the valley entrance to the top of the main valley reaches 499

meters. The average slope gradient of the main valley is 180‰, with a large relative height difference, providing relatively favorable potential energy conditions for the outbreak of debris flows. The vegetation coverage on the south side of the valley slope is greater than 90%, with the vegetation type mainly consisting of trees. On the north side of the valley slope, the vegetation coverage is approximately 80%, mainly consisting of shrubs and herbaceous plants. Due to the uplift of the earth's crust, human activities, and the erosion caused by water flow, a large amount of loose deposit composed of limestone blocks， sand， and cohesive soil has formed in the valley. The loose solid sources are relatively abundant. There are a large number of unconsolidated limestone rocks and gravel at the valley entrance， and a debris fan is developed at the valley entrance.

The valley area of this study region is a typical rainstorm-type debris flow. The cross-sectional shape of the valley is in the form of a "V" shape. The slopes on both sides are steep， with a slope angle mostly above 30°， and the slope gradient is within the range of 300-500‰. The gradually widening valley channel at the valley entrance provides favorable conditions for the accumulation of debris flow solid sources. The overall view of the study area is shown in Figure 1.

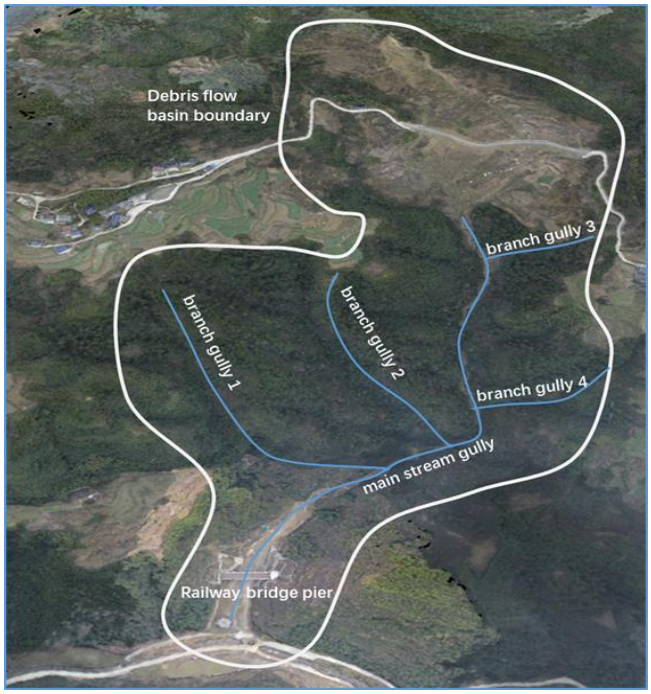

Figure 1: Overview map of the debris flow gully basin in the study area

3. Research Methods

During the simulation of the impact of the debris flow on the dam body, the debris flow slurry will undergo significant deformation. Clearly, the Lagrangian method is unable to meet the requirements, and the meshless processing SPH method is more applicable. However, the deformation of the remaining models is relatively small. If all of them are modeled using SPH particle elements, it will significantly increase the computational cost. To reduce the computational load, the piers, the river channel, and large blocks of stones are modeled using the finite element method. This not only ensures the calculation accuracy but also greatly improves the computational efficiency [6-8].

3.1 The Basic Principle of the SPH Method

3.1.1 Kernel Function Approximation Method

The kernel function approximation method is an integral interpolation method, also known as the continuous integration method [9]. It achieves the conversion of the integral form of any field function through a smooth function [10]. For any function, the following integral expression defined can be adopted [11-13].

$$f(x) = \int_{\Omega} f(x')\delta(x - x')dx' \quad (1)$$

In the formula: f(x) is any function of the three-dimensional coordinate variable x; Ω is the integration domain containing x; δ(x - x') is the Dirac δ function, defined as follows:

$$\delta(x - x') = \begin{cases} 1, x = x' \\ 0, x \neq x' \end{cases} \quad (2)$$

If the δ-function is replaced by the smooth function W(x - x', h), then the integral expression of f(x) can be written as:

$$f(x) = \int_{\Omega} f(x')W(x - x', h)dx' \quad (3)$$

3.1.2 Particle approximation method

Another core idea of the SPH method is the particle approximation method. In the SPH method, the solution domain is represented by a finite number of particles with independent masses and occupying independent spaces. The continuous integral form of a function at any point approximated by a kernel function is transformed into a discrete form of the summation of all particles within a compact support domain. This process is called the particle approximation method. Its expression is:

$$\langle f(x_i) \rangle = \sum_{j=1}^{N} V_i f(x_j) \bullet W_{ij} \quad (4)$$

In the formula: $<f(x_i)>$ represents the particle approximation formula of function f(r) at particle i; the smooth length of the support domain of particle i is h, and there are N neighboring particles. The influence weight of particle j on particle i is $W_{ij}=W(x_i-x_j, h)$; V_j represents the occupied space size of particle j, which represents the length, area, and volume in one-dimensional, two-dimensional, and three dimensional cases respectively.

3.2 Fundamental Theory of FEM

The common algorithms used in FEM mainly include the Lagrange method, the Euler method, and the Arbitrary Lagrangian-Eulerian (ALE) method [14]. The characteristics of each method are as follows:

The Lagrange grid nodes change along with the compression and deformation of the object. Currently, it is widely used in the solution of solid mechanics problems. Its main features are: (1) Since the grid is fixed on the material of the moving object, it is easy to track and determine all the time-domain, motion boundaries and material points on the free surface of the field variables, and it is also easy to apply boundary conditions; (2) Irregular or complex geometric shapes can be handled using irregular grids. Only the grid needs to be arranged within the problem domain, and there are no migration terms in the

related partial differential equations, so the calculation efficiency is high. However, when dealing with large deformation problems, the grid will undergo large deformation and even distortion, resulting in reduced solution accuracy and even failure of the solution [15].

The Euler method can be used for the simulation of large deformation problems in the early stage, but it is difficult to determine the energy and momentum relationship when dealing with deformation boundaries, free surfaces or interface surfaces, and it is difficult to construct grids on irregular or very complex geometric models, and the calculation efficiency of this method is very low [16]. To obtain a more efficient algorithm, the Arbitrary Lagrangian - Eulerian (ALE) method was developed. The grid points of the ALE method can move with the material points, and they can also be fixed in space. This method combines the advantages of Lagrange and Euler, and its grid flexibility is stronger, which can reduce grid distortion. However, for multi-material coupled flows in large flow problems, the ALE method grid cannot replace the simple Euler method grid [17].

4. Establishment of the Calculation Model and Selection of Operating Conditions

4.1 Selection of Calculation Units

This subsection involves three types of units required for the modeling. The bottom of the river is simulated using shell elements, which can enhance the computational efficiency. The abutment dams and large boulders are modeled using solid elements, which are commonly used in three - dimensional solid elements for dynamic analysis. They consist of 8 nodes and support all non-linear analyses, making them suitable for large deformation analysis and controlling the slenderness ratio. The debris flow fluid is simulated using SPH particles [18-20].

4.2 Selection of Material Models

For the riverbed, to improve computational efficiency and prevent penetration during the analysis, the rigid material model from the material library is used for simulation. The boulders are mostly granite, which has small deformation, high strength, and does not need to consider its own deformation during impact and collision, so a rigid material is chosen for simulation. The bridge piers are cast with C30 concrete, as it will undergo elastic-plastic deformation when subjected to impact loads, so the double-linear responsive material model from the material library is selected as the material model for the abutment dams. This material model represents the stress-strain relationship using elasticity and plasticity, and the elastic modulus and Poisson's ratio represent the elastic deformation part. The debris flow fluid is simulated using the Hydrodynamic elastic-plastic fluid dynamics material model. The parameters of the solid material models are as shown in Table 1:

Table 1: Parameters of solid material model

	Density (kg/m^3)	Elastic modulus (Pa)	Poisson's ratio	Yield stress (N)	Shear modulus (Pa)
Riverway	3000	3e10	0.24		
Pier	3000	3e10	0.2	5e6	6.3e9

4.3 Grid Division

Grid division is an important step in model establishment. The selection of grid shape and size will directly affect the efficiency and accuracy of the calculation. The bottom of the river, large boulders, and the dam body are all divided using hexahedral elements. The division size of the river bottom is 500mm, the division size of the bridge piers is 300mm, and the grid of the debris flow slurry is initially divided into 100mm. The grid division results are shown in Figure 2.

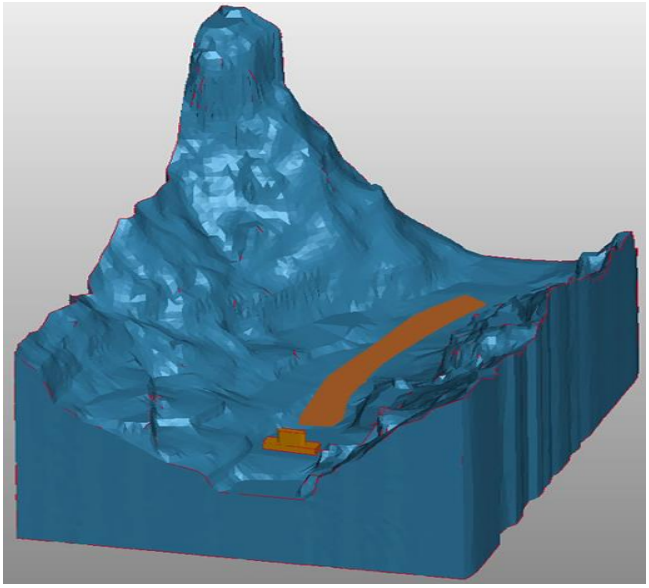

Figure 2: Grid division of debris flow gullies in the study area

5. Analysis of the Dynamic Response of Bridge Piers

5.1 The Dynamics Process of Debris Flow

The overall movement process of the debris flow is shown in Figure 3. As can be seen from Figure 3, the dynamic process of the debris flow impacting the bridge piers consists of four stages: initial contact, accelerated impact, peak impact, and decayed accumulation. The initial contact stage (t=0s), when the front of the debris flow just reaches the bridge pier, the fluid shows a significant non-uniform distribution, and some solid particles begin to collide with the surface of the bridge pier. A short pile-up occurs at the front edge of the bridge pier, and the velocity distribution shows asymmetry. Some fluid begins to flow around. The acceleration impact stage (t=6s), when the main body of the debris flow arrives, the mixture of fluid and solid particles intensifies, forming a strong turbulent structure. Clear vortices and backflows appear around the bridge pier, and some coarse particles briefly accumulate on the downstream-facing surface of the bridge pier, affecting the subsequent movement path of the fluid. The peak impact stage (t=12s), when the debris flow flow reaches its maximum, the fluid shows a high-concentration solid-liquid two-phase flow characteristic, and the flow around the bridge pier and the impact range expand. The collision frequency of solid particles increases, and the fluid kinetic energy reaches its peak transfer to the bridge pier, and a tail flow zone may appear behind the bridge pier, forming a local deposition. The decayed accumulation stage (t=18s), after the main body of the debris flow passes, the fluid kinetic energy gradually weakens, but some fine particle suspensions continue to flow.

The accumulated solid substances around the bridge pier change the local terrain and affect the subsequent movement direction of the fluid, and may form a new secondary flow path.

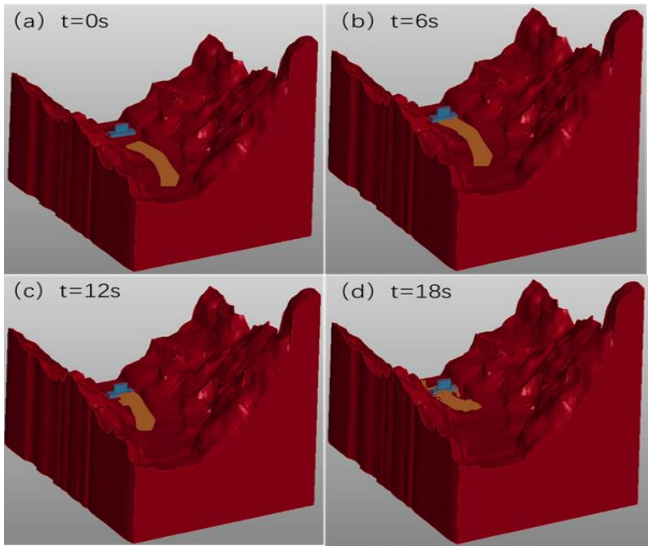

Figure 3: The overall dynamic process of debris flow

5.2 Overall Impact Force Analysis of the Bridge Piers

5.2.1 Occurs once every 20 years

The overall impact force of the bridge piers due to debris flow is shown in Figure 4. As can be seen from the figure, at t=6.5s, the debris flow begins to come into contact with the bridge piers, and at t=20s, the impact force reaches the main peak of 2320kN. This indicates that the debris flow has the characteristics of strong suddenness and rapid impact, which is consistent with the instantaneous dynamic load characteristics generated by the high-density solid substances entrained in the debris flow. At t=21s, the debris flow slurry continuously rises, converting kinetic energy into potential energy, reducing the speed and the impact force. This reflects the energy dissipation caused by the deposition of coarse particles in the debris flow or the increase in fluid viscosity resistance, as well as the vibration damping effect of the bridge pier structure. At t=23s, the impact force drops to 920kN and continues to impact until the end of 40s, indicating that there is a long-term dragging force during the continuous action of the debris flow, related to the viscous effect of the fine particle slurry at the tail of the flow or the static pressure generated by the accumulated debris around the bridge pier.

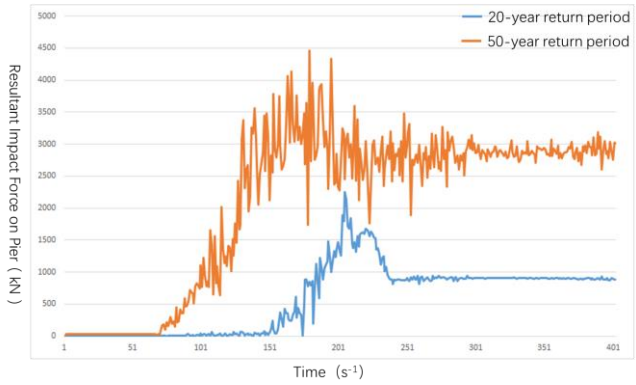

Figure 4: Resultant Impact Force on Pier

Debris flow has the characteristics of high density, large impact force and strong destructive power. Its load time history curve usually shows an initial instantaneous peak impact in the initial stage, and then gradually decays due to the deposition of solid substances in the flow, energy dissipation and structural damping effect. However, there may still be some residual load at the tail. As a lateral load-bearing structure, the dynamic response characteristics of the bridge pier mainly manifest as the instantaneous shear and bending moment effects during the peak impact stage, which may cause local plastic deformation or cracking. During the load decay stage, the vibration frequency and damping characteristics of the bridge pier will significantly affect its dynamic stability, and the residual load may exacerbate the long-term fatigue damage of the structure or the risk of foundation erosion.

5.2.2 Occurs once every 50 years

The overall impact force of the bridge piers due to debris flow is shown in Figure 4. The energy change stage and trend of the debris flow overall energy are basically consistent with those of the 20-year event. The maximum load value of the bridge pier under the 50-year flood condition is approximately 4500kN, which is significantly higher than that of the 20-year event, indicating the significant amplification effect of extreme hydrological events on the structural load. The peak occurrence time (t=25s) is consistent with the peak stage of the flood process, which is in line with the time-varying characteristics of the hydraulic impact load. The curve shows a non-linear steep increase trend in the ascending segment (t=0s-t=25s), reflecting the coupling effect of the dynamic water pressure caused by the increasing water flow velocity and the debris flow impact. The descending segment (t=25s-t=40s) has a slower decaying rate, indicating that the damping characteristics of the bridge pier structure have a certain alleviating effect on resisting the debris flow impact.

5.3 Bridge Pier Energy Analysis

The overall kinetic energy time course of the debris flow can be divided into three stages: the kinetic energy growth stage, the kinetic energy decay stage, and the re-activation stage. During the kinetic energy growth stage, the debris flow begins to accumulate kinetic energy due to the difference in elevation of the channel, and then reaches the peak kinetic energy. The accumulation of kinetic energy of the debris flow in this stage is mainly influenced by factors such as the elevation difference of the channel and the friction coefficient at the bottom of the channel. In the kinetic energy decay stage, due to the impact between the debris flow and the bridge piers, the plastic deformation of the bridge piers and the internal friction of the debris flow cause the kinetic energy to be converted into other forms such as heat energy, ultimately resulting in the start of the decrease in the kinetic energy of the debris flow. The peak kinetic energy of a 50-year debris flow is approximately 6500 kJ, and the residual kinetic energy after decay is approximately 2000 kJ. The peak kinetic energy of a 20-year debris flow is approximately 4500 kJ, and the residual kinetic energy after decay is approximately 1000 kJ. In the re-activation stage, due to the existence of elevation difference in the river channel and the inability of the bridge piers to completely consume the kinetic energy of the debris flow, the debris flow re-activates and continues to move

downstream. The overall kinetic energy time history curve of the debris flow is shown in Figure 5.

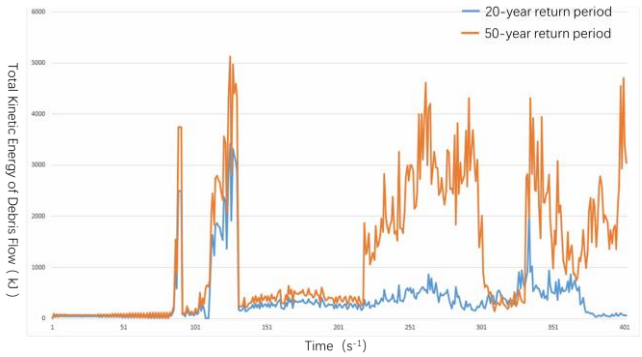

Figure 5: Total Kinetic Energy of Debris Flow

The overall internal energy time course of the bridge piers can be divided into three stages: the initial energy surge stage, the rapid attenuation stage, and the slow attenuation stage. In the initial energy surge stage, due to the instantaneous impact of the debris flow, the kinetic energy of the bridge piers suddenly increases. The energy forms include elastic strain energy generated by the deformation of the pier body and kinetic energy generated by the overall vibration. In the rapid attenuation stage, due to the impact of the debris flow, micro cracks or local yielding occur in the concrete of the bridge piers. Through the combined action of external damping such as plastic deformation energy dissipation, internal damping of the structure, friction of the foundation soil, and friction of the debris flow residue, the energy rapidly attenuates. The 50-year recurrence debris flow reaches the stable stage at around 5.5 seconds, with kinetic energy of approximately 7000 kJ. After a slow attenuation of 23 seconds, it gradually rises. The 20-year recurrence debris flow reaches the peak kinetic energy of approximately 6000 kJ at 15 seconds, and after attenuation, the residual kinetic energy is approximately 1000 kJ. In the slow attenuation stage, the remaining energy is gradually released in the form of elastic vibration, and the attenuation rate decreases, indicating that the system is approaching stability. The overall internal energy curve of the bridge piers is shown in Figure 5.

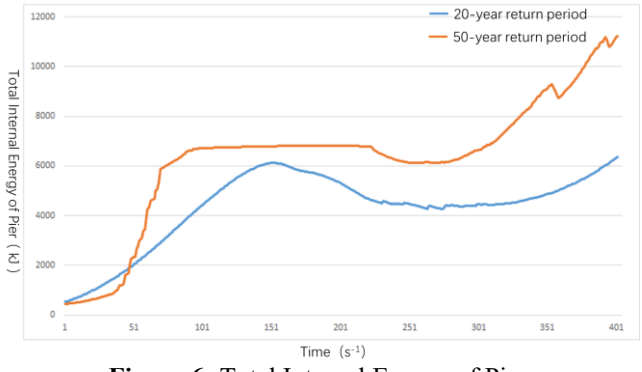

Figure 6: Total Internal Energy of Pier

6. Conclusion

This study is based on the SPH-FEM coupling numerical simulation method, and systematically investigates the dynamic response characteristics of railway bridge piers under the impact of debris flows. The study adopts a method combining theoretical analysis, numerical simulation, and parametric research, deeply exploring the interaction mechanism between debris flows and bridge piers, and reaching the following conclusions:

1) This study established an SPH-FEM coupling model considering the solid-liquid two-phase characteristics of debris flows. Through the refinement of grid division technology, multi-scale simulations of the bridge pier structure (300mm grid) and the debris flow fluid (100mm particles) were achieved. Particularly, the bilinear synchronous hardening model accurately described the elastic-plastic behavior of concrete materials, and the Hydrodynamic model was combined to simulate the high-density fluid characteristics of debris flows, providing a reliable numerical analysis framework for complex fluid-solid coupling problems.

2) The results show that the debris flow impact process has obvious three-stage characteristics: 1) The initial contact stage, where the debris flow front contacts the bridge pier, the fluid shows non-uniform distribution, and the impact force rises rapidly; 2) The peak impact stage, where the debris flow body arrives, the bridge pier bears the maximum dynamic load; 3) The decay and accumulation stage, where the impact force gradually decays, but the residual load continues to act. This dynamic load characteristic is significantly different from traditional static loads and regular dynamic loads.

3) The study found that the kinetic energy of debris flows is mainly transformed through three pathways: structural elastic strain energy, plastic deformation dissipation, and other forms of energy dissipation. In terms of structural response characteristics, the stress distribution and deformation mode are significantly different from static conditions. Concrete materials exhibit nonlinear mechanical behavior under impact loads, and this characteristic requires special attention in structural design.

References

[1] Tayyebi S M, Pastor M, Stickle M M. Two-phase SPH numerical study of pore-water pressure effect on debris flows mobility: Yu Tung debris flow[J]. Computers and Geotechnics, 2021, 132: 103973.

[2] Denlinger R P, Iverson R M. Flow of variably fluidized granular masses across three-dimensional terrain: 2. Numerical predictions and experimental tests[J]. Journal of Geophysical Research: Solid Earth, 2001, 106(B1): 553-566.

[3] Luo G, Zhao Y, Shen W, et al. Dynamics of bouldery debris flow impacting onto rigid barrier by a coupled SPH-DEM-FEM method [J]. Computers and Geotechnics, 2022, 150:104936.

[4] Kwan J S H, Sze E H Y, Lam C. Finite element analysis for rockfall and debris flow mitigation works[J]. Canadian Geotechnical Journal, 2019, 56(9): 1225-1250.

[5] Clough R W. The finite element in plane strain analysis[C]. Proc. 2nd ASCE Conf, on Electric computation, 1960: 345-378.

[6] Wang W, Chen G, Han Z, et al. 3D numerical simulation of debris-flow motion using SPH method incorporating non-Newtonian fluid behavior[J]. Natural Hazards, 2016, 81: 1981-1998.

[7] Minatti L, Pasculli A. SPH numerical approach in modelling 2D muddy debris flow[C]. International Conference on Debris-Flow Hazards Mitigation: Mechanics, Prediction, and Assessment, Proceedings, 2011: 467-475.
[8] Huang Y, Yiu J, Pappin J, et al. Numerical investigation of landslide mobility and debris resistant flexible barrier with LS-DYNA[C]. Proceedings of the 13th international LS-DYNA users conference, 2014: 8-10.
[9] Cascini L, Cuomo S, Pastor M, et al. SPH-FDM propagation and pore water pressure modelling for debris flows in flume tests[J]. Engineering Geology, 2016, 213: 74-83.
[10] Monaghan J J. Smoothed particle hydrodynamics[J]. Reports on progress in physics, 2005, 68(8): 1703.
[11] Gingold R A, Monaghan J J. Smoothed particle hydrodynamics: theory and application to non-spherical stars[J]. Monthly notices of the royal astronomical society, 1977, 181(3): 375-389.
[12] Monaghan J J. An introduction to SPH[J]. Computer physics communications, 1988, 48(1): 89-96.
[13] Herreros M I, Mabssout M. A two-steps time discretization scheme using the SPH method for shock wave propagation[J]. Computer Methods in Applied Mechanics and Engineering, 2011, 200(21-22): 1833-1845.
[14] Jeong S, Lee K. Analysis of the impact force of debris flows on a check dam by using a coupled Eulerian - Lagrangian (CEL) method[J]. Computers and Geotechnics, 2019, 116: 103214.
[15] Liu C, Yu Z, Zhao S. A coupled SPH-DEM-FEM model for fluid-particle-structure interaction and a case study of Wenjia gully debris flow impact estimation[J]. Landslides, 2021, 18: 2403-2425.
[16] Liu C, Liang L. A coupled SPH-DEM-FEM approach for modeling of debris flow impacts on flexible barriers[J]. Arabian Journal of Geosciences, 2022, 15(5): 420.
[17] Li B, Wang C, Li Y, et al. Dynamic response analysis of retaining dam under the impact of solid-liquid two-phase debris flow based on the coupled SPH-DEM-FEM method [J]. Geofluids, 2020, 2020: 1-12.
[18] Qing Y Z, Ming X Z, Dan H. Numerical simulation of impact and entrainment behaviors of debris flow by using SPH-DEM-FEM coupling method[J]. Open Geosciences, 2022, 14(1): 1020-1047.
[19] Trujillo-Vela M G, Galindo-Torres S A, Zhang X, et al. Smooth particle hydrodynamics and discrete element method coupling scheme for the simulation of debris flows[J]. Computers and Geotechnics, 2020, 125: 103669.
[20] Martinez C E, Miralles-Wilhelm F, Garcia Martinez R. Quasi-three dimensional two-phase debris flow model accounting for boulder transport[J]. Italian Journal of Engineering Geology and Environment-Book, 2011, 3: 457-466.